

Active control of the resistive wall mode with power saturation

Li Li, Yue Liu, and Yueqiang Liu

Citation: *Phys. Plasmas* **19**, 012502 (2012); doi: 10.1063/1.3672512

View online: <http://dx.doi.org/10.1063/1.3672512>

View Table of Contents: <http://pop.aip.org/resource/1/PHPAEN/v19/i1>

Published by the [American Institute of Physics](#).

Related Articles

Density gradient effects in weakly nonlinear ablative Rayleigh-Taylor instability
Phys. Plasmas **19**, 012706 (2012)

Surpassing one x-ray photon per electron in nonlinear Thomson scattering in 180° geometry
Phys. Plasmas **19**, 013111 (2012)

Symmetries of resistive two-fluid magnetohydrodynamics under reversals of toroidal field, current, and rotation
Phys. Plasmas **19**, 014505 (2012)

The effect of elementary reactions on solitary waves in dusty plasmas
Phys. Plasmas **19**, 014503 (2012)

Adiabatic nonlinear waves with trapped particles. II. Wave dispersion
Phys. Plasmas **19**, 012103 (2012)

Additional information on *Phys. Plasmas*

Journal Homepage: <http://pop.aip.org/>

Journal Information: http://pop.aip.org/about/about_the_journal

Top downloads: http://pop.aip.org/features/most_downloaded

Information for Authors: <http://pop.aip.org/authors>

ADVERTISEMENT



HAVE YOU HEARD?

Employers hiring scientists
and engineers trust
physicstodayJOBS



<http://careers.physicstoday.org/post.cfm>

Active control of the resistive wall mode with power saturation

Li Li,^{1,a)} Yue Liu,¹ and Yueqiang Liu²

¹*School of Physics and Optoelectronic Technology, Dalian University of Technology, Dalian, 116024, People's Republic of China*

²*Euratom/CCFE Fusion Association, Culham Science Centre, Abingdon OX14 3DB, United Kingdom*

(Received 7 September 2011; accepted 14 November 2011; published online 9 January 2012)

An analytic model of non-linear feedback stabilization of the resistive wall mode is presented. The non-linearity comes from either the current or the voltage saturation of the control coil power supply. For the so-called flux-to-current control, the current saturation of active coils always results in the loss of control. On the contrary, the flux-to-voltage control scheme tolerates certain degree of the voltage saturation. The minimal voltage limit is calculated, below which the control will be lost. © 2012 American Institute of Physics. [doi:10.1063/1.3672512]

I. INTRODUCTION

In high pressure, high bootstrap fraction tokamak fusion plasma scenarios, the operational limit is often set by the resistive wall mode (RWM), which becomes unstable as soon as the plasma pressure exceeds the Troyon no-wall beta limit,¹ according to the ideal magnetohydrodynamic (MHD) theory. Because of its global mode structure, this mode can hardly enter into a non-linear phase and saturate by itself, before causing the major disruption of the plasma. Therefore, the RWM stability physics and control has been a subject of extensive study during recent years, in particular, in view of its importance for the steady state scenarios in ITER² and possibly also in the future fusion reactor devices.

Even though recent theory^{3–6} and experiments^{7,8} seem to suggest an important stabilizing effect on the RWM, due to drift kinetic resonances between the mode and the thermal or energetic particles, a complete suppression of the mode remains fragile, especially for ITER.^{9,10} This is partially due to the uncertainty in the prediction of the toroidal plasma flow speed in ITER, partially due to the experimental fact that a marginally stable RWM can be easily triggered by other MHD modes, by external (error) fields, or by energetic particles.^{11–13} It appears that active control of the RWM remains an essential aspect for the ITER steady state scenarios.

The RWM is also often present in the reversed field pinch (RFP) devices, where the mode onset often results in an earlier termination of the discharge. Unlike in tokamaks, the RWM stabilization by subsonic plasma flow,¹⁴ or by drift kinetic effects,¹⁵ does not seem to be effective. Therefore, feedback stabilization of the RWM is critical for the operation of the (thin shell) RFP devices.

Extensive theory^{16–22} and experimental^{23–31} work has been carried out to study the active control of the RWM, in both tokamak and RFP devices. Even though the power saturation of the feedback system is often the case in experiments, very few theoretical work has been performed

addressing this issue. Perhaps one exception is Ref. 32, where the RWM feedback with the voltage saturation is numerically solved as a non-linear control problem. Most of the modeling work predicting the RWM control performance in ITER assumes a linear closed loop, without considering the power saturation.^{33–35} On the other hand, the in-vessel coils in the present ITER design, which have been proposed both for the RWM control, have limits both in the coil current (96 kA-turn), and in the power supply voltage (144 V). Moreover, the same coil system is shared by the edge localized mode (ELM) control. Therefore, the actual current and voltage limits for the RWM control should be even lower. It is critical that the RWM control system to be designed to meet these limits.

This work attempts to make a systematic investigation of the power supply saturation problem for the RWM control, by considering an analytically tractable RWM control model. Our results, though qualitative, show interesting aspects of the non-linear control of the RWM, due to the current or voltage saturation of the active magnetic coils. Quantitative prediction of the power saturation limits, as well as the closed loop behavior in the presence of saturation, requires detailed numerical modeling, which will be our future work.

Section II describes the control model adopted in this work. With this simple cylindrical model, we aim at a systematic exploitation of various possible feedback configurations. Section III briefly describes the open loop and the linear closed loop results. The main results are reported in Sec. IV, where the non-linear behavior of the closed loop, in the presence of the control signal saturation, is investigated. Section V concludes the paper.

II. THE CONTROL MODEL

We shall consider a single harmonic, cylindrical model for the RWM control, following earlier analytic work.^{36–38} We develop a compact formalism that includes a rather complete set of feedback configurations. This will facilitate our further study of the linear and non-linear control.

^{a)}Electronic mail: lil@mail.dlut.edu.cn.

We start with the vacuum solution in a straight cylinder. Denoting the radial position of the plasma boundary, the (thin) resistive wall, and the active coil as a, r_w, r_f , respectively. The vacuum solution, for the perturbed radial magnetic flux ψ , can be written as

$$\psi = \psi_p \left(\frac{r}{a}\right)^{-m} + \psi_f \left(\frac{r}{r_f}\right)^m + \psi_w \left(\frac{r}{r_w}\right)^m,$$

in the region between the plasma boundary and the first conducting structure (either wall or active coil). Here, ψ_p, ψ_f, ψ_w is the flux contribution produced by the perturbed plasma current, the active coil current, and the wall current, at the radial location a, r_f, r_w , respectively. $m > 0$ is the poloidal harmonic number. (The toroidal harmonic number is assumed to be $n \neq 0$ but formally does not enter into the formulation.)

The flux in the vacuum region between the wall and the active coil is

$$\psi = \psi_p \left(\frac{r}{a}\right)^{-m} + \psi_f \left(\frac{r}{r_f}\right)^{-\nu m} + \psi_w \left(\frac{r}{r_w}\right)^{\nu m},$$

where $\nu = 1$ if the active coil is located inside the wall ($r_f < r_w$, internal active coil), and $\nu = -1$ if the active coil is located outside the wall ($r_f > r_w$, external active coil).

Finally, the vacuum solution outside the last conducting structure is

$$\psi = \psi_p \left(\frac{r}{a}\right)^{-m} + \psi_f \left(\frac{r}{r_f}\right)^{-m} + \psi_w \left(\frac{r}{r_w}\right)^{-m}.$$

We note that the above representation of the perturbed flux, in the vacuum regions, automatically satisfies the continuity condition of the poloidal flux across the conductor interfaces.

The solution inside the plasma depends on the equilibrium current and pressure profiles. However, for the purpose of the control study, the coupling of the linear plasma dynamics to the “external” world can be specified via a single quantity

$$\frac{r\psi'}{\psi} \Big|_a = c_0, \quad (1)$$

calculated at the plasma-vacuum interface. The prime here denotes the radial derivative. Note that c_0 is a quantity fully determined by the inner plasma solution (eventually by the equilibrium current and pressure profiles), and hence, c_0 is not affected by the wall current nor the active coil current. Moreover, c_0 can be related to the open loop growth rate of the resistive wall mode, which will be treated as a known quantity in this work.

Assuming a thin wall approximation, the perturbed flux satisfies a well known jump condition

$$\frac{\partial\psi}{\partial t} \Big|_{r_w} = \frac{1}{\tau_w} r[\psi'] \Big|_{r_w}, \quad (2)$$

where $\tau_w = \mu_0 \sigma r_w d$ is the so-called wall time, with σ, d being the wall conductivity and thickness, respectively. $[\psi']$

denotes the jump of the radial derivative of ψ across the wall surface.

Before proceeding with specifications of the sensor signals and the feedback logics, we note that the boundary condition (1), together with the vacuum solution just outside the plasma, couples ψ_p, ψ_f , and ψ_w independent of the control configuration

$$\psi_p = \frac{m - c_0}{m + c_0} \left(\frac{a}{r_f}\right)^m \psi_f + \frac{m - c_0}{m + c_0} \left(\frac{a}{r_w}\right)^m \psi_w. \quad (3)$$

We shall consider both flux and voltage sensors. For the flux sensor, the sensor signal y can be either the total radial flux at the wall $y = \psi(r = r_w)$, or the radial derivative of the poloidal flux from the inner side of the wall $y = -r_w \psi'(r = r_w^-)$. The latter is equivalent to the so-called internal poloidal sensor. In either case, taking into account Eq. (3), the flux sensor signal can be generally written as

$$y = \alpha \psi_f + \beta \psi_w,$$

where the parameters α and β will depend on the sensor type. Similarly, the voltage sensors can be generally represented as

$$y = \alpha \frac{d\psi_f}{dt} + \beta \frac{d\psi_w}{dt}.$$

The control signal u can be either the current I_f or voltage V_f of the active coil. For the current control, we assume $u = \psi_f$, utilizing the fact that $\psi_f = L_f I_f$, with L_f being the self-inductance of the active coil. For the voltage control, we have

$$u = V_f = \frac{d\psi}{dt} \Big|_{r_f} + \frac{2m}{\tau_f} \psi_f,$$

where $\tau_f \equiv 2mL_f/R_f$, with R_f being the coil's resistance, characterizes the response time of the active coil. By definition, the total voltage applied to the active coil consists of the inductive and the resistive parts. Note that the inductive voltage is calculated as the time derivative of the total flux ψ through the coil.

We consider a feedback scheme that allows saturation of the control signal u

$$u = \text{sat}\{-Ky, u_{\text{sat}}\} \equiv \begin{cases} -Ky, & \text{if } |Ky| < u_{\text{sat}}, \\ \text{sign}(-Ky)u_{\text{sat}}, & \text{if } |Ky| \geq u_{\text{sat}}, \end{cases} \quad (4)$$

where K is the controller gain, and u_{sat} is the maximal control signal, which the power supply can provide.

III. OPEN LOOP DYNAMICS AND CLOSED LOOP WITHOUT SATURATION

Combining the wall equation (2) with Eq. (3), we obtain

$$(AB + B^{-\nu}) \frac{d\psi_f}{dt} + (A + 1) \frac{d\psi_w}{dt} + \frac{2m}{\tau_w} \psi_w = 0, \quad (5)$$

where we have introduced two notations

$$A \equiv \frac{m - c_0}{m + c_0} \left(\frac{a}{r_w} \right)^{2m}, \quad B \equiv \left(\frac{r_w}{r_f} \right)^m.$$

Note that $B > 1$ for $\nu = 1$, and $B < 1$ for $\nu = -1$, by our definitions.

The open loop of the current control scheme assumes $u = \psi_f = 0$. Substituting this condition into Eq. (5), we find the growth rate γ_0 of the RWM in the absence of any feedback system

$$\gamma_0 = -\frac{2m}{\tau_w} \frac{1}{A + 1} = -\frac{2m}{\tau_w} \frac{m + c_0}{(m + c_0) + (m - c_0)(a^{2m}/r_w^{2m})}.$$

In further study, we shall assume that $\gamma_0 > 0$, and hence, $A + 1 < 0$.

The open loop of the voltage control is different from that of the current control, due to the inductive and resistive response of the active coil to the plasma and wall currents, even in the absence of the feedback. In this case, the active coil effectively acts as a second resistive wall. The open loop equation for the coil is derived as

$$u = V_f = (AB^2 + 1) \frac{d\psi_f}{dt} + (AB + B^{-\nu}) \frac{d\psi_w}{dt} + \frac{2m}{\tau_f} \psi_f = 0. \quad (6)$$

Equations (5) and (6) jointly determine the open loop eigenvalues $\gamma_{1,2}^0$, satisfying a quadratic equation

$$\left[(AB^2 + 1)(A + 1) - (AB + B^{-\nu})^2 \right] \gamma^2 + 2m \left(\frac{AB^2 + 1}{\tau_w} + \frac{A + 1}{\tau_f} \right) \gamma + \frac{4m^2}{\tau_w \tau_f} = 0. \quad (7)$$

It can be easily shown that, as long as τ_f remains finite, $\left[(AB^2 + 1)(A + 1) - (AB + B^{-\nu})^2 \right] < 0$ independent of the coil-wall configuration, resulting in one unstable open loop root, and one stable root. At $\tau_f = \infty$, the active coil effectively acts as a perfectly conducting wall. The open loop does not have unstable roots in this case, if $AB^2 + 1 < 0$. The last condition is always satisfied for internal active coils. In further study, we shall assume that this condition is also satisfied for external active coils. This gives a limitation on how far the active coil can be placed outside the wall

$$r_f < \left(1 + \frac{2m}{\gamma_0 \tau_w} \right)^{1/(2m)} r_w. \quad (8)$$

For a typical RWM, the normalized open loop growth rate $\gamma_0 \tau_w$ is of order unity, the above constraint on the active coil's position is not very stringent. For instance, for the $m = 2$ mode, r_f should be within $1.49r_w$; for the $m = 3$ mode, r_f should be within $1.38r_w$.

Now we turn to the sensor type specification. Using Eq. (3) and the sensor definition, we find that for radial sensors, $\alpha = AB + B^{-\nu}$, $\beta = A + 1$; for internal poloidal sensors, $\alpha = m(AB + \nu B^{-\nu})$, $\beta = m(A - 1)$. One can also define an external poloidal sensor as $y = -r\psi'|_{r_w+}$ and find $\alpha = m(AB + \nu B^{-\nu})$, $\beta = m(A + 1)$. However, we shall not consider the external poloidal sensors for the RWM control, due to its poor performance.³⁷ Moreover, at sufficiently large feedback gain, the external poloidal sensors often cause a second instability of the closed loop system. Independent of the sensor type, α and β are always negative.

Because of the two choices for the sensor signal (flux or voltage), and two choices for the control signal (current or voltage), we have four possible combinations for the control logic. Below we give a systematic, but brief study for each of the cases.

A. Flux-to-current control

The linear control logic reads

$$\psi_f = -K(\alpha\psi_f + \beta\psi_w).$$

Combining with the wall equation (5), we obtain the linear growth rate of the closed loop

$$\gamma^c = -\frac{2m}{\tau_w} \frac{1 + \alpha K}{(A + 1) + DK}, \quad (9)$$

where $D \equiv \alpha(A + 1) - \beta(AB + B^{-\nu})$. It is clear that $D = 0$ for radial sensors, as well as for internal poloidal sensors combined with external active coils ($\nu = -1$). For internal poloidal sensors with internal active coils ($\nu = 1$), $D = 2m(AB + B^{-\nu}) < 0$.

Equation (9) shows that the closed loop will be linearly stable, as soon as the (proportional) feedback gain exceeds a critical value $K > K_{cr} \equiv -1/\alpha > 0$.

We mention that a PID controller $K = K_p + K_d \frac{d}{dt} + K_i \int dt$ with proportional, derivative, and integral actions are often considered for the RWM feedback. The derivative gain helps to increase the phase lead of the closed loop system but does not change the stability margin of an unstable root with vanishing real frequency, at which $\frac{d}{dt} = 0$. The integral gain introduces a phase lag (as well as an additional root) to the closed loop. It can often affect the stability of the closed loop. For simplicity, we will not consider the integral action in this work, but pointing out that a pure integral action converts the voltage sensor into the flux sensor.

B. Flux-to-voltage control

This is perhaps the most interesting and useful control logic for the RWM stabilization

$$V_f = (AB^2 + 1) \frac{d\psi_f}{dt} + (AB + B^{-\nu}) \frac{d\psi_w}{dt} + \frac{2m}{\tau_f} \psi_f = -K(\alpha\psi_f + \beta\psi_w).$$

The linear eigenvalues $\gamma_{1,2}^c$ of the closed loop satisfy a quadratic equation

$$\begin{aligned} & \left[(AB^2 + 1)(A + 1) - (AB + B^{-\nu})^2 \right] \gamma^2 \\ & + \left(2m \frac{AB^2 + 1}{\tau_w} + 2m \frac{A + 1}{\tau_f} + DK \right) \gamma \\ & + \frac{2m}{\tau_w} \left(\frac{2m}{\tau_f} + \alpha K \right) = 0. \end{aligned} \quad (10)$$

Since $(AB^2 + 1) < 0$, $(A + 1) < 0$, $D \leq 0$, examination of the sign of the coefficients from the above quadratic equation reveals that both roots become negative, as soon as the feedback gain exceeds a critical value $K > K_{cr} \equiv -2m/(\tau_f \alpha)$.

Equation (10) also shows that, at sufficiently large control gain, the two stable roots become complex conjugates. The only exception is the internal active coil combined with the internal poloidal sensor, for which the two roots always remain real.

C. Voltage-to-voltage control

The control logic in this case is

$$V_f = -K \left(\alpha \frac{d\psi_f}{dt} + \beta \frac{d\psi_w}{dt} \right).$$

The eigenvalue equation for the closed loop reads

$$\begin{aligned} & \left[(AB^2 + 1)(A + 1) - (AB + B^{-\nu})^2 + DK \right] \gamma^2 \\ & + 2m \left(\frac{AB^2 + 1}{\tau_w} + \frac{A + 1}{\tau_f} + \frac{\alpha K}{\tau_w} \right) \gamma + \frac{4m^2}{\tau_w \tau_f} = 0. \end{aligned}$$

Examining the signs of the coefficients of the above equation, we find that full stabilization is not possible with a proportional controller. However, since a pure integral action converts the voltage sensor into the flux sensor, it can stabilize the closed loop.

D. Voltage-to-flux control

The control logic is

$$\psi_f = -K \left(\alpha \frac{d\psi_f}{dt} + \beta \frac{d\psi_w}{dt} \right).$$

The resulting eigenvalue equation for the linear closed loop becomes

$$DK\gamma^2 + \left(A + 1 + \frac{2m}{\tau_w} \alpha K \right) \gamma + \frac{2m}{\tau_w} = 0.$$

With radial sensors or internal poloidal sensors combined with external coils, $D = 0$, and hence, there is only a single root, which is unstable. The marginal stability is achieved at infinite proportional gain $K_{cr} = +\infty$.

With internal poloidal sensors and internal active coils, $D < 0$, and hence, no full stabilization is possible unless the feedback gain becomes infinite.

IV. NON-LINEAR CONTROL WITH POWER SUPPLY SATURATION

The results from Sec. III show that, with a finite proportional feedback gain, and without the control signal saturation, the full stabilization of the closed loop can be achieved only for the flux-to-current and the flux-to-voltage control schemes. For the other two schemes (voltage-to-voltage and voltage-to-flux), the closed loop is always unstable without saturation and will certainly be unstable with the control signal saturation.

Therefore, the question is whether the flux-to-current and the flux-to-voltage control schemes, which are stable at $K > K_{cr}$ without saturation, can still maintain the stability in the presence of the current or voltage saturation.

A. Flux-to-current control

The answer for the flux-to-current control is relatively simple. Suppose that the open loop system starts the time evolution at $t = 0$, with the initial value $\psi_w(t = 0) = \psi_0$, $\psi_f(t = 0) = 0$. At the time moment $t = t_1$, the loop is closed. If at the time interval $[t_1, t_1 + \delta t]$, with arbitrarily small δt , the current saturates at the power supply limit, i.e., $u = \psi_f = (\pm)u_{sat}$, we have $d\psi_f/dt = 0$. The wall equation (5) converts into the open loop equation, meaning that the control is completely lost. Therefore, at least in this ideal situation, the flux-to-current control scheme cannot tolerate the current saturation.

On the other hand, if no saturation occurs at the time interval $[t_1, t_1 + \delta t]$, the time evolution of the closed loop can be easily constructed. For instance, the sensor signal $y(t)$ becomes

$$y(t \geq t_1) = -\psi_0 \frac{\beta}{\alpha} \frac{K}{K - K_{cr}} e^{\gamma_0 t_1} e^{\gamma^c (t - t_1)},$$

where γ^c is calculated according to Eq. (9). Since $\gamma^c < 0$ at $K > K_{cr}$, the sensor signal $y(t)$ always decays to zero, after the feedback is switched on. Therefore, if the current saturation is not achieved at the time moment t_1 , it will never be achieved in any further time moment $t > t_1$. Consequently, the closed loop proceeds as a linear current control scheme without saturation.

B. Flux-to-voltage control

The situation with the flux-to-voltage control is more interesting. We shall proceed by constructing the time evolution solutions for three cases: (i) the open loop solution at the time interval $[0, t_1]$; (ii) the closed loop solution without saturation, at a time interval $[t_2, t_3]$; (iii) the closed loop solution with the voltage saturation, at a time interval $[t_4, t_5]$. The final time trace will be a proper combination of these solutions (i.e., a proper choice of time moments t_2, t_3, \dots).

The two coupled open loop equations can be written in a matrix form

$$\mathbf{E} \frac{d\mathbf{X}}{dt} = \mathbf{F}_0 \mathbf{X},$$

where

$$\mathbf{E} \equiv \begin{bmatrix} AB^2 + 1 & AB + B^{-\nu} \\ AB + B^{-\nu} & A + 1 \end{bmatrix},$$

$$\mathbf{F}_0 \equiv \begin{bmatrix} -2m/\tau_f & 0 \\ 0 & -2m/\tau_w \end{bmatrix}, \quad \mathbf{X} \equiv \begin{bmatrix} \psi_f \\ \psi_w \end{bmatrix}. \quad (11)$$

Since all the coefficients of the above system are time-independent, the solution is easily constructed from the open loop eigenvectors and eigenvalues. Assume that the eigenvector \mathbf{X}_1^0 and \mathbf{X}_2^0 correspond to the eigenvalues γ_1^0 and γ_2^0 , respectively. For definiteness, we assume $\gamma_1^0 > 0$ and $\gamma_2^0 < 0$. The open loop solution is

$$\mathbf{X}(t) = \mathbf{X}^0 \mathbf{I}^0(t) (\mathbf{X}^0)^{-1} \mathbf{X}_0,$$

where $\mathbf{X}^0 \equiv [\mathbf{X}_1^0 \ \mathbf{X}_2^0]$, $\mathbf{X}_0 = \mathbf{X}(t=0) = [0 \ \psi_0]^T$ is the initial value. \mathbf{I}^0 is a diagonal matrix

$$\mathbf{I}^0(t) \equiv \begin{bmatrix} e^{\gamma_1^0 t} & 0 \\ 0 & e^{\gamma_2^0 t} \end{bmatrix}. \quad (12)$$

The eigenmatrix \mathbf{X}^0 , and its inverse, can be easily constructed

$$\mathbf{X}^0 = \begin{bmatrix} \gamma_1^0(A+1) + 2m/\tau_w & -\gamma_2^0(A+1) - 2m/\tau_w \\ -\gamma_1^0(AB+B^{-\nu}) & \gamma_2^0(AB+B^{-\nu}) \end{bmatrix}, \quad (13)$$

$$(\mathbf{X}^0)^{-1} = c^0 \begin{bmatrix} \gamma_2^0(AB+B^{-\nu}) & \gamma_2^0(A+1) + 2m/\tau_w \\ \gamma_1^0(AB+B^{-\nu}) & \gamma_1^0(A+1) + 2m/\tau_w \end{bmatrix}, \quad (14)$$

where $c^0 \equiv \tau_w/(2m)/[(AB+B^{-\nu})(\gamma_2^0 - \gamma_1^0)]$.

The matrix equation for the saturated closed loop is similar to that of the open loop

$$\mathbf{E} \frac{d\mathbf{X}}{dt} = \mathbf{F}_0 \mathbf{X} + \mathbf{U},$$

where $\mathbf{U} \equiv [(\pm)u_{\text{sat}} \ 0]^T$. The solution at the time interval $[t_4, t_5]$ is

$$\mathbf{X}(t) = \mathbf{X}^0 \mathbf{I}^0(t-t_4) (\mathbf{X}^0)^{-1} (\mathbf{X}_4 + \mathbf{F}_0^{-1} \mathbf{U}) - \mathbf{F}_0^{-1} \mathbf{U},$$

where $\mathbf{X}_4 \equiv \mathbf{X}(t=t_4)$ is the solution at the time moment t_4 .

Finally, the matrix equation for the closed loop without saturation reads

$$\mathbf{E} \frac{d\mathbf{X}}{dt} = \mathbf{F}_c \mathbf{X},$$

where

$$\mathbf{F}_c = \mathbf{F}_0 - K \begin{bmatrix} \alpha & \beta \\ 0 & 0 \end{bmatrix}. \quad (15)$$

Denoting $\gamma_{1,2}^c$ the two roots of the linear closed loop, the eigenmatrix of the closed loop can be easily constructed, together with its inverse matrix

$$\mathbf{X}^c = \begin{bmatrix} \gamma_1^c(A+1) + 2m/\tau_w & -\gamma_2^c(A+1) - 2m/\tau_w \\ -\gamma_1^c(AB+B^{-\nu}) & \gamma_2^c(AB+B^{-\nu}) \end{bmatrix}, \quad (16)$$

$$(\mathbf{X}^c)^{-1} = c^c \begin{bmatrix} \gamma_2^c(AB+B^{-\nu}) & \gamma_2^c(A+1) + 2m/\tau_w \\ \gamma_1^c(AB+B^{-\nu}) & \gamma_1^c(A+1) + 2m/\tau_w \end{bmatrix}, \quad (17)$$

where $c^c \equiv \tau_w/(2m)/[(AB+B^{-\nu})(\gamma_2^c - \gamma_1^c)]$. The closed loop solution at the time interval $[t_2, t_3]$ is

$$\mathbf{X}(t) = \mathbf{X}^c \mathbf{I}^c(t-t_2) (\mathbf{X}^c)^{-1} \mathbf{X}_2,$$

where $\mathbf{X}_2 \equiv \mathbf{X}(t=t_2)$.

In order to understand the closed loop behavior, we are mostly interested in finding two voltage limits V_f^{max} and V_f^{min} . V_f^{max} is the peak voltage of the closed loop without any saturation condition. Obviously, if the power supply voltage limit u_{sat} is greater than V_f^{max} , no saturation will ever occur during the feedback operation.

On the other hand, we shall prove that there exists a minimal voltage level V_f^{min} , such that if $u_{\text{sat}} < V_f^{\text{min}}$, the closed loop flux-to-voltage control will saturate all the time, resulting in the loss of the stability for the mode control (even when $K > K_{\text{cr}}$).

We first find the V_f^{max} value. For this, we connect the open loop solution (i) with the linear closed loop solution (ii) at $t = t_1 = t_2$. The solution $\mathbf{X}(t)$ should be continuous across the connection point, yielding

$$V_f(t \geq t_1) = -K[\alpha \ \beta] \mathbf{X}^c \mathbf{I}^c(t-t_1) (\mathbf{X}^c)^{-1} \mathbf{X}^0 \mathbf{I}^0(t_1) (\mathbf{X}^0)^{-1} \mathbf{X}_0.$$

A lengthy but straightforward calculation eventually gives

$$V_f(t \geq t_1) = C_f [p e^{\gamma_1^c(t-t_1)} - q e^{\gamma_2^c(t-t_1)}],$$

where $C_f \equiv -K\psi_0/[(AB+B^{-\nu})(\gamma_2^0 - \gamma_1^0)(\gamma_2^c - \gamma_1^c)]$, $p \equiv (D\gamma_1^c + \alpha/\hat{\tau}_w)(a\gamma_2^c + b)$, $q \equiv (D\gamma_2^c + \alpha/\hat{\tau}_w)(a\gamma_1^c + b)$, and $a \equiv \Delta_1 + \hat{\tau}_w \hat{A} \Delta_2$, $b \equiv (1/\hat{\tau}_w - d\hat{\tau}_w)\Delta_1/\hat{A} + \Delta_2$, $d \equiv (\gamma_1^0 \hat{A} + 1/\hat{\tau}_w)(\gamma_2^0 \hat{A} + 1/\hat{\tau}_w)$, $\Delta_1 = \exp(\gamma_1^0 t_1) - \exp(\gamma_2^0 t_1)$, $\Delta_2 \equiv \gamma_2^0 \exp(\gamma_1^0 t_1) - \gamma_1^0 \exp(\gamma_2^0 t_1)$. We have also introduced two new notations $\hat{A} \equiv A + 1$, $\hat{\tau}_w \equiv \tau_w/(2m)$.

For definiteness, we assume that $\psi_0 > 0$, $\gamma_2^0 < 0 < \gamma_1^0$, $\gamma_2^c < \gamma_1^c < 0$. It is easy to see that $C_f > 0$, $\Delta_1 > 0$, $\Delta_2 < 0$, $a > 0$. Utilizing Eq. (7), it can be shown that $b < 0$. Note that here we derive V_f^{max} for real $\gamma_{1,2}^c$. At sufficiently large feedback gain for the flux-to-voltage control, $\gamma_{1,2}^c$ become complex conjugates. Our final results are valid also for the latter case.

First, we notice that $p - q = (Db - \alpha\hat{\tau}_w a)(\gamma_1^c - \gamma_2^c) > 0$, and hence, $V_f(t_1) > 0$. Furthermore, it can be shown that $p\gamma_1^c - q\gamma_2^c > 0$ for the three feedback configurations where $D = 0$ (radial sensors with internal or external active coils, internal poloidal sensors with external active coils). Therefore, $dV_f(t)/dt > 0$ at $t = t_1$. This, combined with the fact that $V_f(t)$ vanishes at $t = \infty$, shows the existence of a maximal value of V_f at a time moment $t > t_1$, for the case with $D = 0$. This maximum can be easily calculated as

$$V_f^{\max}|_{D=0} = C_f \left[p \left(\frac{q\gamma_2^c}{p\gamma_1^c} \right)^{\gamma_1^c/(\gamma_1^c-\gamma_2^c)} - q \left(\frac{q\gamma_2^c}{p\gamma_1^c} \right)^{\gamma_2^c/(\gamma_1^c-\gamma_2^c)} \right].$$

For the last case of $D < 0$ (internal poloidal sensors with internal active coils), it can be shown that $dV_f/dt < 0$ for all $t \geq t_1$, indicating that V_f^{\max} is achieved at the time moment $t = t_1$

$$V_f^{\max}|_{D<0} = C_f(p - q).$$

Now we turn to the calculation of V_f^{\min} . We shall *a-priori* assume that $V_f^{\min} < V_f(t_1)$. This assumption will be rigorously proven after the V_f^{\min} value is calculated. We connect the open loop solution (i) with the closed loop saturation solution (iii) at $t = t_1 = t_4$. Note that, since $V_f(t_1) > 0$ is solely determined by the open loop, we can assume that $u_{\text{sat}} > 0$. Introducing a function $g(t \geq t_1) \equiv -ky(t)/u_{\text{sat}}$, where $y = \alpha\psi_f + \beta\psi_w$, we try to find a minimal value of u_{sat} (i.e. V_f^{\min}), that leads to $g(t) \geq 1$ for all $t \geq t_1$. Note that by connecting the solutions (i) and (iii), we have implicitly assumed that $g(t = t_1) \geq 1$. The function $g(t)$ is straightforwardly calculated

$$\begin{aligned} g(t \geq t_1) &= -\frac{K}{u_{\text{sat}}} [\alpha \beta] [\mathbf{X}^0 \mathbf{I}^0(t) (\mathbf{X}^0)^{-1} \mathbf{X}_0 + \mathbf{X}^0 \mathbf{I}^0(t - t_1) \\ &\quad \times (\mathbf{X}^0)^{-1} \mathbf{F}_0^{-1} [u_{\text{sat}} \ 0]^T - \mathbf{F}_0^{-1} [u_{\text{sat}} \ 0]^T], \\ &= -Kc^0 (D\gamma_1^0 + \alpha/\hat{\tau}_w) \\ &\quad \times \left[\frac{\psi_0}{u_{\text{sat}}} (\hat{A}\gamma_2^0 + 1/\hat{\tau}_w) e^{\gamma_1^0 t_1} - \hat{\tau}_f \gamma_2^0 (AB + B^{-\nu}) \right] \\ &\quad \times e^{\gamma_1^0 (t-t_1)} + Kc^0 (D\gamma_2^0 + \alpha/\hat{\tau}_w) \\ &\quad \times \left[\frac{\psi_0}{u_{\text{sat}}} (\hat{A}\gamma_1^0 + 1/\hat{\tau}_w) e^{\gamma_2^0 t_1} - \hat{\tau}_f \gamma_1^0 (AB + B^{-\nu}) \right] \\ &\quad \times e^{\gamma_2^0 (t-t_1)} - \alpha \hat{\tau}_f K, \\ &= g_1 e^{\gamma_1^0 (t-t_1)} + g_2 e^{\gamma_2^0 (t-t_1)} - \alpha \hat{\tau}_f K, \end{aligned}$$

where $\hat{\tau}_f \equiv \tau_f/(2m)$, and g_1 and g_2 are defined according to the above equations. The sign of the last term

$$G \equiv \frac{\psi_0}{u_{\text{sat}}} (\hat{A}\gamma_2^0 + 1/\hat{\tau}_w) e^{\gamma_1^0 t_1} - \hat{\tau}_f \gamma_2^0 (AB + B^{-\nu})$$

from the g_1 coefficient determines whether $g(t)$ will be larger than 1 for all time $[t_1, \infty)$, or $g(t) \geq 1$ only at a finite time interval. In the former case, the control will be lost due to the saturation, and the closed loop will eventually become unstable. In the latter case, the saturation does not lead to the loss of the stability of the closed loop.

Indeed, if $G < 0$, we have $g_1 < 0$. Since $g(t_1) \geq 1$, and $\gamma_1^0 > 0, \gamma_2^0 < 0$, it is clear that at some time moment, $g(t)$ will be less than one. If $G > 0$ instead, we have $g_1 > 0$. There are two possible cases. In the first case, $D < 0$, it can be shown that $g_2 > 0$. The last term of $g(t)$, $-\alpha \hat{\tau}_f K \geq 1$, as soon as $K \geq K_{\text{cr}}$. Therefore, $g(t)$ will be greater than 1 for all t . In the second case, $D = 0$, g_1 is still positive, but g_2 becomes negative. However, since the $g_1 \exp[\gamma_1^0 (t - t_1)]$ term increases with time, the $g_2 \exp[\gamma_2^0 (t - t_1)]$ vanishes towards

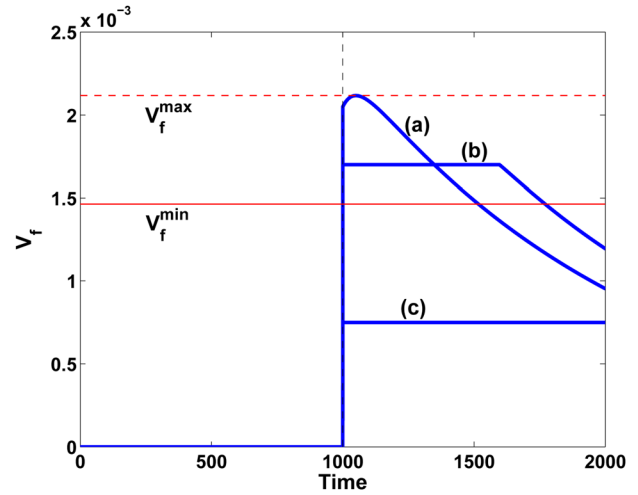


FIG. 1. (Color online) Comparison of three voltage limits (a) $u_{\text{sat}} > V_f^{\max}$ (no saturation), (b) $V_f^{\min} < u_{\text{sat}} = 1.7 \times 10^{-3} < V_f^{\max}$ (with saturation), and (c) $u_{\text{sat}} = 7.5 \times 10^{-4} < V_f^{\min}$ (with full saturation). The radial flux sensor and internal active coil are considered, with $r_f = 1.1a, r_w = 1.2a$, $\tau_w = \tau_f = 1000\tau_A, m = 2, \gamma_0\tau_w = 5$.

zero, and the fact that $g(t_1) \geq 1$, we conclude that $g(t)$ will be larger than 1 for all time.

The above discussions lead to the calculation of the minimal voltage limit V_f^{\min} , defined as the solution of $G = 0$

$$V_f^{\min} = \frac{\psi_0 \gamma_2^0 (A + 1) + 1/\hat{\tau}_w}{\hat{\tau}_f \gamma_2^0 (AB + B^{-\nu})} e^{\gamma_1^0 t_1},$$

below which the closed loop will lose the stability. It is not difficult to show that $V_f^{\min} < V_f(t_1)$.

It is interesting to note that, unlike V_f^{\max} , V_f^{\min} does not depend on the feedback gain. Moreover, it does not depend on whether the radial or internal poloidal sensors are used for the closed loop.

We show two examples of the impact of the voltage saturation on the feedback performance. The first example (Figs. 1–3) employs the *radial flux* sensor-to-voltage control scheme, whilst the second (Figs. 4–6) employs the *internal poloidal flux* sensor-to-voltage scheme. The internal active coil is used in both examples. As can be easily understood from the above analytic results, the feedback behavior with external active coils is similar to that of the internal coil case with radial sensors, regardless whether radial or internal poloidal sensor is used.

Figure 1 compares three cases. In case (a), the voltage limit u_{sat} in the feedback loop is set above the maximal achievable voltage V_f^{\max} during the linear closed loop, i.e., without saturation. In case (b), the voltage limit u_{sat} is chosen between the lower limit V_f^{\min} and the upper limit V_f^{\max} . The voltage is saturated for a period of time but eventually recovers a linear control phase without the loss of stability. This is also evident from the time trace of the radial flux from the coil and the wall, shown in Fig. 2(b).

The lower voltage limit V_f^{\min} is the “hard” limit for saturation, in the sense that the control cannot be recovered as soon as $u_{\text{sat}} < V_f^{\min}$. The voltage saturates forever (case (c) in

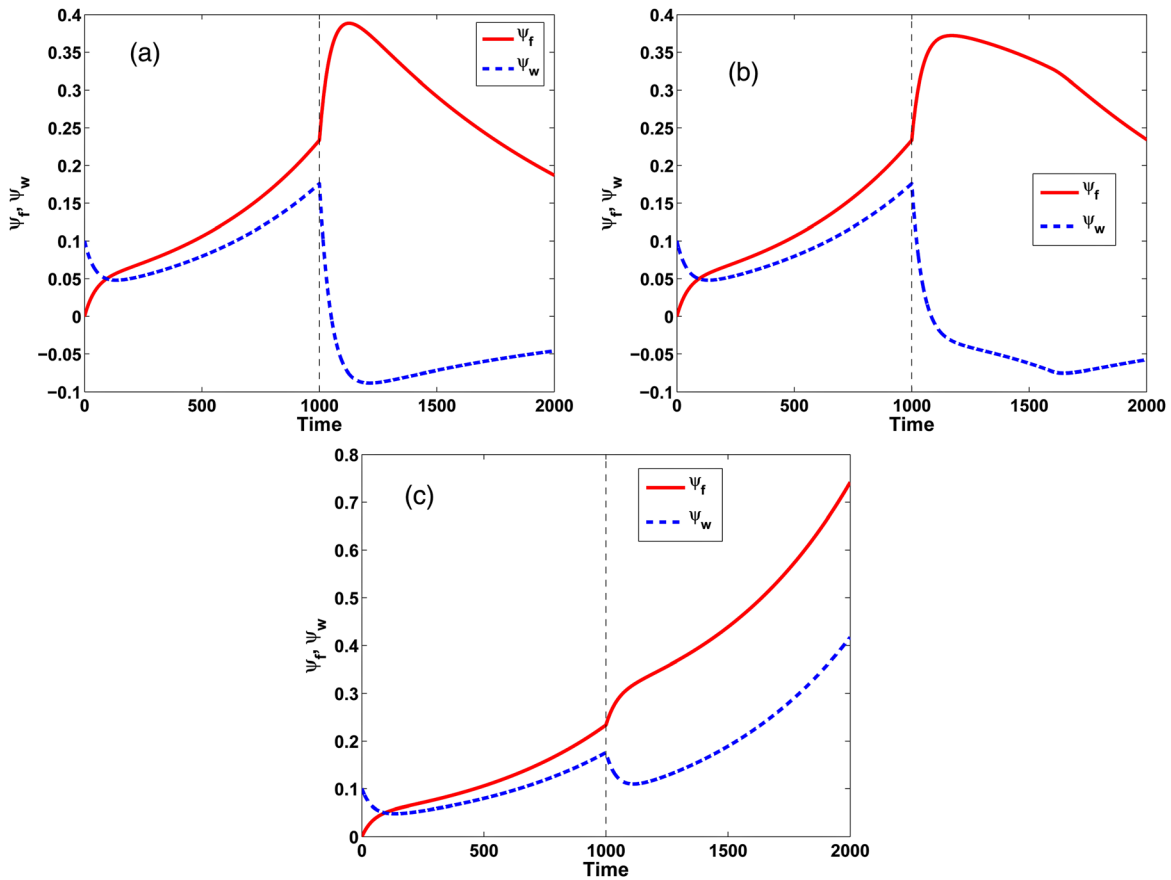


FIG. 2. (Color online) The time evolution of the radial flux due to the active coil (ψ_f) and the resistive wall (ψ_w), corresponding to the three cases (a)–(c) from Fig. 1. The feedback is switched on at $t_1 = 1000\tau_A$, with a proportional gain $K = 1.5K_{cr}$.

Fig. 1), and consequently the closed loop eventually becomes unstable, as shown by Fig. 2(c).

Figure 3 plots both the lower and the upper limits of the voltage saturation, as a function of the closed loop gain. Whilst the lower limit does not depend on the gain value, the upper limit is nearly a linear function of gain. No saturation occurs if the maximal voltage u_{max} of the control power sup-

ply exceeds V_f^{max} . No stable control can be achieved if u_{max} is below V_f^{min} . In the region between the V_f^{min} and V_f^{max} curves, the closed loop remains stable despite of the voltage saturation.

Figures 4–6 show the feedback behavior using the internal poloidal flux sensor instead of the radial flux. The results

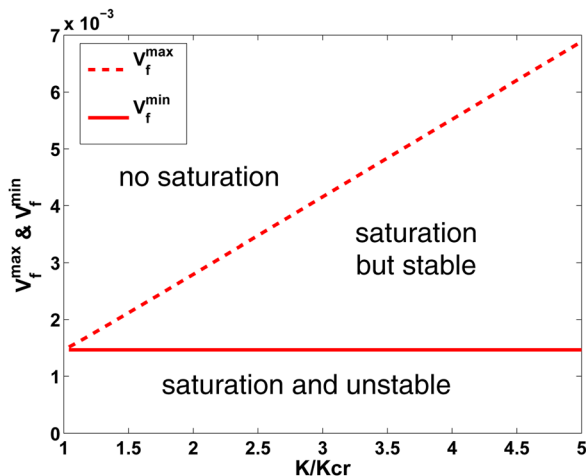


FIG. 3. (Color online) The lower (V_f^{min}) and upper (V_f^{max}) limits for the voltage saturation, versus the proportional feedback gain. The configuration is the same as that from Fig. 1.

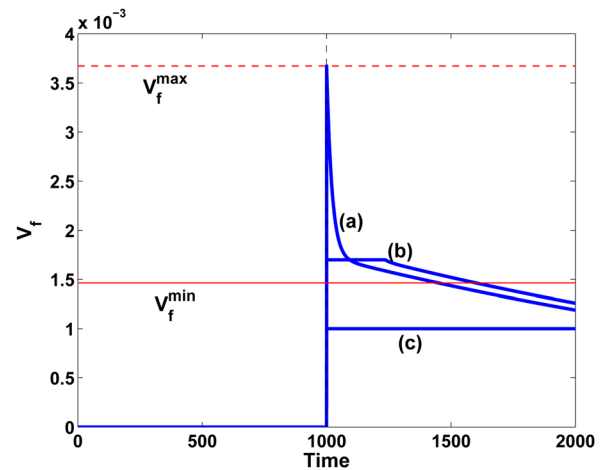


FIG. 4. (Color online) Comparison of three voltage limits (a) $u_{sat} > V_f^{max}$ (no saturation), (b) $V_f^{min} < u_{sat} = 1.7 \times 10^{-3} < V_f^{max}$ (with saturation), and (c) $u_{sat} = 10^{-3} < V_f^{min}$ (with full saturation). The internal poloidal flux sensor and internal active coil are considered, with $r_f = 1.1a, r_w = 1.2a, \tau_w = \tau_f = 1000\tau_A, m = 2, \gamma_0\tau_w = 5$.

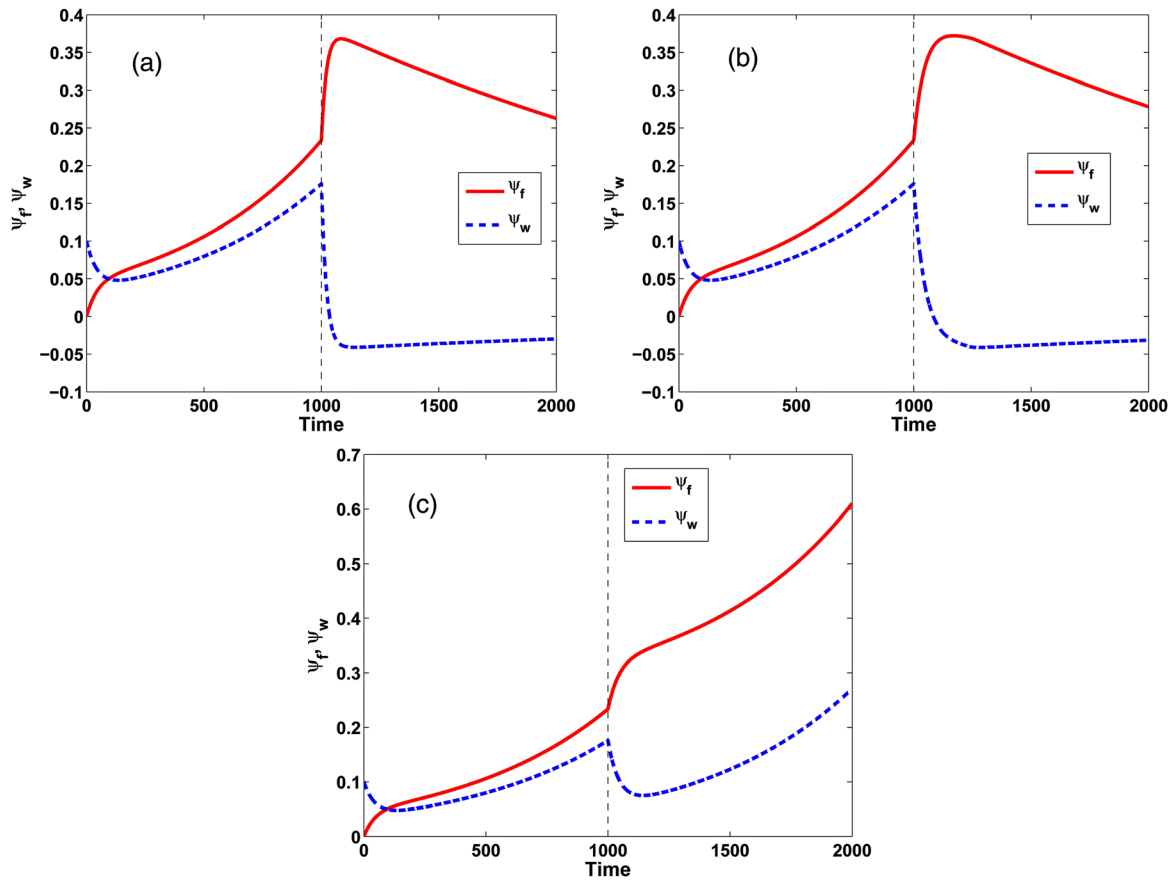


FIG. 5. (Color online) The time evolution of the radial flux due to the active coil (ψ_f) and the resistive wall (ψ_w), corresponding to the three cases (a)–(c) from Fig. 4. The feedback is switched on at $t_1 = 1000\tau_A$, with a proportional gain $K = 1.5K_{cr}$.

are similar, except for the control voltage time trace. With the internal poloidal sensor (and the internal active coil), the voltage peaking of the control coil always occurs at the moment when the feedback is switched on. This is not the case with radial sensors. Such a difference has been pointed out in the above analytic derivations.

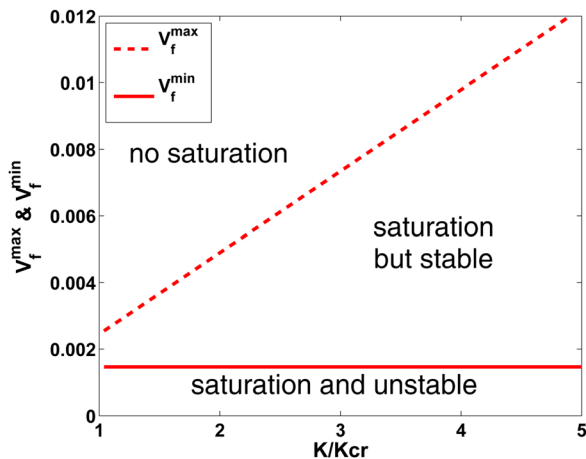


FIG. 6. (Color online) The lower (V_f^{\min}) and upper (V_f^{\max}) limits for the voltage saturation, versus the proportional feedback gain. The configuration is the same as that from Fig. 4.

V. CONCLUSION AND DISCUSSION

We have performed a systematic investigation of the resistive wall mode control using magnetic coils, based on an analytic cylindrical model. The key aspect is the non-linearity of the control model, introduced by the saturation of the power supply.

Without the power saturation and with a simple controller (a combination of proportional and derivative actions), only two control schemes can give full stabilization of mode at sufficiently large feedback gains, namely the flux-to-current control and the flux-to-voltage control schemes.

For these two control schemes, the problem of the power supply saturation can be studied, when the linear (i.e., without saturation) closed loop is stable. We find that the current control scheme, with a proportional controller, cannot tolerate the saturation of the control coil current. The closed loop becomes unstable as soon as the active coils reach the current limit. This statement is valid for an ideal situation, where the current saturation is caused by a single unstable mode only. In the presence of multiple (stable and unstable) modes, it may happen that the current saturation is caused by the controller response to the stable mode(s), whilst the control of the unstable mode is not lost. A multi-mode control model needs to be developed to investigate this, which is beyond the scope of the present study. More advanced

controllers may help to improve the current control scheme with saturation. A good understanding will most likely require numerical simulations. Though for a bang-bang controller, it can be demonstrated that the current saturation still leads to the loss of control.

On the contrary, the voltage control scheme allows a certain degree of saturation, without the loss of the closed loop stability. There exists, however, a critical value of the voltage limit, below which the closed loop will eventually become unstable. Moreover, we have shown that, in our model, this lower threshold of the voltage saturation level does not depend on the feedback gain, nor on the choice of the sensor type.

ACKNOWLEDGMENTS

This work is supported by NSFC under Grant Nos. 10675029, 11075030 and National Basic Research Program of China under Grant Nos. 2008CB717801, 2008CB787103, 2009GB105004, 2010GB106002.

- ¹F. Troyon, R. Gruber, H. Saurenmann, S. Semenzato, and S. Succi, *Plasma Phys. Controlled Fusion* **26**, 209 (1984).
- ²R. Aymar, P. Barabaschi, and Y. Shimomura, *Plasma Phys. Controlled Fusion* **44**, 519 (2002).
- ³B. Hu and R. Betti, *Phys. Rev. Lett.* **93**, 105002 (2004).
- ⁴Y. Q. Liu, M. S. Chu, I. T. Chapman, and T. C. Hender, *Phys. Plasmas* **15**, 112503 (2008).
- ⁵I. T. Chapman, M. P. Gryaznevich, C. G. Gimblett, T. C. Hender, D. F. Howell, Y. Q. Liu, S. D. Pinches, and JET EFDA Contributors, *Plasma Phys. Controlled Fusion* **51**, 055015 (2009).
- ⁶G. Z. Hao, Y. Q. Liu, A. K. Wang, H. B. Jiang, Gaimin Lu, H. D. He, and X. M. Qiu, *Phys. Plasmas* **18**, 032513 (2011).
- ⁷H. Reimerdes, A. M. Garofalo, G. L. Jackson, M. Okabayashi, E. J. Strait, M. S. Chu, Y. In, R. J. La Haye, M. J. Lanctot, Y. Q. Liu, G. A. Navratil, W. M. Solomon, H. Takahashi, and R. J. Groebner, *Phys. Rev. Lett.* **98**, 055001 (2007).
- ⁸M. Takechi, G. Matsunaga, N. Aiba, T. Fujita, T. Ozeki, Y. Koide, Y. Sakamoto, G. Kurita, A. Isayama, Y. Kamada, and JT-60 Team, *Phys. Rev. Lett.* **98**, 055002 (2007).
- ⁹Y. Q. Liu, M. S. Chu, I. T. Chapman, and T. C. Hender, *Nucl. Fusion* **49**, 035004 (2009).
- ¹⁰J. W. Berkery, S. A. Sabbagh, H. Reimerdes, R. Betti, B. Hu, R. E. Bell, S. P. Gerhardt, J. Manickam, and M. Podesta, *Phys. Plasmas* **17**, 082504 (2010).
- ¹¹G. Matsunaga, N. Aiba, K. Shinohara, Y. Sakamoto, A. Isayama, M. Takechi, T. Suzuki, N. Oyama, N. Asakura, Y. Kamada, and T. Ozeki (JT-60 Team), *Phys. Rev. Lett.* **103**, 045001 (2009).
- ¹²M. Okabayashi, G. Matsunaga, M. Takechi, J. S. deGrassie, W. W. Heidbrink, Y. In, Y. Q. Liu, E. J. Strait, N. Asakura, R. Budny, G. Jackson, J. Hanson, R. J. La Haye, M. J. Lanctot, J. Manickam, H. Reimerdes, and K. Shinohara, *Phys. Plasmas* **18**, 056112 (2011).
- ¹³G. Z. Hao, A. K. Wang, Y. Q. Liu, and X. M. Qiu, *Phys. Rev. Lett.* **107**, 015001 (2011).
- ¹⁴S. C. Guo, J. P. Freidberg, and R. Nachtrieb, *Phys. Plasmas* **6**, 3868 (1999).
- ¹⁵D. Yadykin, Y. Q. Liu, R. Paccagnella, *Plasma Phys. Controlled Fusion* **53**, 085024 (2011).
- ¹⁶Y. Q. Liu and A. Bondeson, *Phys. Rev. Lett.* **84**, 907 (2000).
- ¹⁷Y. Q. Liu, A. Bondeson, C. M. Fransson, B. Lennartson, and C. Breitholtz, *Phys. Plasmas* **7**, 3681 (2000).
- ¹⁸C. M. Fransson, B. Lennartson, C. Breitholtz, A. Bondeson, and Y. Q. Liu, *Phys. Plasmas* **7**, 4143 (2000).
- ¹⁹J. Bialek, A. H. Boozer, M. E. Mauel, and G. A. Navratil, *Phys. Plasmas* **8**, 2170 (2001).
- ²⁰M. S. Chu, M. S. Chance, A. H. Glasser, and M. Okabayashi, *Nucl. Fusion* **43**, 441 (2003).
- ²¹E. Strumberger, P. Merkel, M. Sempf, and S. Guenter, *Phys. Plasmas* **15**, 056110 (2008).
- ²²Z. R. Wang and S. C. Guo, *Nucl. Fusion* **51**, 053004 (2011).
- ²³E. D. Fredrickson, J. Bialek, A. M. Garofalo, L. C. Johnson, R. J. La Haye, E. A. Lazarus, J. Manickam, G. A. Navratil, M. Okabayashi, J. T. Scoville, and E. J. Strait, *Plasma Phys. Controlled Fusion* **43**, 313 (2001).
- ²⁴A. M. Garofalo, M. S. Chu, E. D. Fredrickson, M. Gryaznevich, T. H. Jensen, L. C. Johnson, R. J. La Haye, G. A. Navratil, M. Okabayashi, J. T. Scoville, E. J. Strait, A. D. Turnbull, and DIII-D Team, *Nucl. Fusion* **41**, 1171 (2001).
- ²⁵M. Okabayashi, J. Bialek, M. S. Chance, M. S. Chu, E. D. Fredrickson, A. M. Garofalo, M. Gryaznevich, R. E. Hatcher, T. H. Jensen, L. C. Johnson, R. J. La Haye, E. A. Lazarus, M. A. Makowski, J. Manickam, G. A. Navratil, J. T. Scoville, E. J. Strait, A. D. Turnbull, and M. L. Walker, *Phys. Plasmas* **8**, 2071 (2001).
- ²⁶E. J. Strait, J. Bialek, N. Bogatu, M. Chance, M. S. Chu, D. Edgell, A. M. Garofalo, G. L. Jackson, T. H. Jensen, L. C. Johnson, J. S. Kim, R. J. La Haye, G. Navratil, M. Okabayashi, H. Reimerdes, J. T. Scoville, A. D. Turnbull, M. L. Walker, and the DIII-D Team, *Nucl. Fusion* **43**, 430 (2003).
- ²⁷E. J. Strait, J. M. Bialek, I. N. Bogatu, M. S. Chance, M. S. Chu, D. H. Edgell, A. M. Garofalo, G. L. Jackson, R. J. Jayakumar, T. H. Jensen, O. Katsuro-Hopkins, J. S. Kim, R. J. La Haye, L. L. Lao, M. A. Makowski, G. A. Navratil, M. Okabayashi, H. Reimerdes, J. T. Scoville, A. D. Turnbull, and DIII-D Team, *Phys. Plasmas* **11**, 2505 (2004).
- ²⁸C. Cates, M. Shilov, M. E. Mauel, G. A. Navratil, D. Maurer, S. Mukherjee, D. Nadle, J. Bialek, and A. Boozer, *Phys. Plasmas* **7**, 3133 (2000).
- ²⁹P. R. Brunzell, D. Yadykin, D. Gregoratto, R. Paccagnella, T. Bolzonella, M. Cavinato, M. Cecconello, J. R. Drake, A. Luchetta, G. Manduchi, G. Marchiori, L. Marrelli, P. Martin, A. Masiello, F. Milani, S. Ortolani, G. Spizzo, and P. Zanca, *Phys. Rev. Lett.* **93**, 225001 (2004).
- ³⁰J. R. Drake, P. R. Brunzell, D. Yadykin, M. Cecconello, J. A. Malmberg, D. Gregoratto, R. Paccagnella, T. Bolzonella, G. Manduchi, L. Marrelli, S. Ortolani, G. Spizzo, P. Zanca, A. Bondeson, and Y. Q. Liu, *Nucl. Fusion* **45**, 557 (2005).
- ³¹M. Okabayashi, N. Bogatu, T. Bolzonella, M. S. Chance, M. S. Chu, A. M. Garofalo, R. Hatcher, Y. In, G. L. Jackson, J. S. Kim, R. J. La Haye, M. J. Lanctot, Y. Q. Liu, T. C. Luce, J. Manickam, L. Marrelli, P. Martin, G. A. Navratil, H. Reimerdes, E. J. Strait, H. Takahashi, and A. S. Welander, *Nucl. Fusion* **49**, 125003 (2009).
- ³²Y. Q. Liu, A. Bondeson, D. Gregoratto, C. M. Fransson, Y. Gribov, R. Paccagnella, *Nucl. Fusion* **44**, 77 (2004).
- ³³Y. Q. Liu, A. Bondeson, Y. Gribov, and A. Polevoi, *Nucl. Fusion* **44**, 232 (2004).
- ³⁴Y. Q. Liu, M. S. Chu, W. F. Guo, F. Villone, R. Albanese, G. Ambrosino, M. Baruzzo, T. Bolzonella, I. T. Chapman, A. M. Garofalo, C. G. Gimblett, R. J. Hastie, T. C. Hender, G. L. Jackson, R. J. La Haye, M. J. Lanctot, Y. In, G. Marchiori, M. Okabayashi, R. Paccagnella, M. Furno Palumbo, A. Pironti, H. Reimerdes, G. Rubinacci, A. Soppelsa, E. J. Strait, S. Ventre, and D. Yadykin, *Plasma Phys. Controlled Fusion* **52**, 104002 (2010).
- ³⁵F. Villone, Y. Q. Liu, G. Rubinacci, and S. Ventre, *Nucl. Fusion* **50**, 125011 (2010).
- ³⁶V. D. Pustovitov, *Plasma Phys. Rep.* **27**, 195 (2001).
- ³⁷A. Bondeson, Y. Q. Liu, D. Gregoratto, Y. Gribov, and V. D. Pustovitov, *Nucl. Fusion* **42**, 768 (2002).
- ³⁸Y. Q. Liu, *Plasma Phys. Controlled Fusion* **48**, 969 (2006).